Non-linear analyses model for composite box-girders with corrugated steel webs under torsion

Hee-Jung Ko[1], Jiho Moon[1], Yong-Woo Shin[2] and Hak-Eun Lee[*1]

*[1]School of Civil, Environmental & Architectural Engineering, Korea University,
145 Anam-ro, Seongbuk-gu, Seoul 136-701, South Korea*
[2]Civil Engineering Team, Daewoo E&C, 57 Sinmunno 1-ga, Jongno-gu, Seoul 110-713, South Korea

Abstract.   A composite box-girder with corrugated steel webs has been used in civil engineering practice as an alternative to the conventional pre-stressed concrete box-girder because of several advantages, such as high shear resistance without vertical stiffeners and an increase in the efficiency of pre-stressing due to the accordion effect. Many studies have been conducted on the shear buckling and flexural behavior of the composite box-girder with corrugated steel webs. However, the torsional behavior is not fully understood yet, and it needed to be investigated. Prior study of the torsion of the composite box-girder with corrugated steel webs has been developed by assuming that the concrete section is cracked prior to loading and doesn't have tensile resistance. This results in poor estimation of pre-cracking behaviors, such as initial stiffness. To overcome this disadvantage of the previous analytical model, an improved analytical model for torsion of the composite box-girder with corrugated steel webs was developed considering the concrete tension behavior in this study. Based on the proposed analytical model, a non-linear torsional analysis program for torsion of the composite box-girder with corrugated steel webs was developed and successfully verified by comparing with the results of the test. The proposed analytical model shows that the concrete tension behavior has significant effect on the initial torsional stiffness and cracking torsional moment. Finally, a simplified torsional moment-twist angle relationship of the composite box-girder with corrugated steel webs was proposed based on the proposed analytical model.

Keywords: torsion; corrugated steel webs; composite structure; non-linear analysis; box-girder bridge

1. Introduction

The composite box-girder with corrugated steel webs shown in Fig. 1 has been used since late 1980s as an alternative to the conventional pre-stressed concrete box-girder because of several advantages. First, the corrugated steel webs have large out-of-plane bending resistance and shear stiffness because the inclined panels serve as a vertical stiffener. Second, most of the normal stresses are taken by the steel flange and concrete slabs because of the accordion effect (Hamilton 1993), and this leads to an increase in the efficiency of the pre-stressing. Further, the weight of box-girders can be reduced by replacing the concrete webs, which account for about 10 to 30% of the dead load in pre-stressed concrete box-girder bridges, with corrugated steel webs (Yi *et al.* 2008).

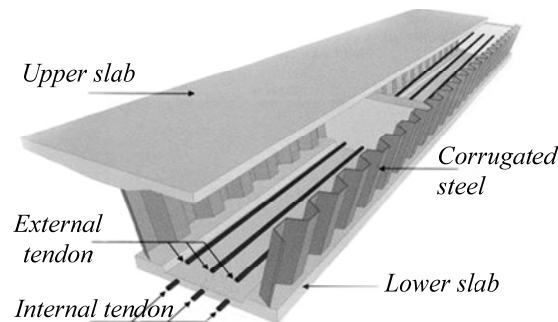∗Corresponding author, Professor, E-mail: helee@korea.ac.kr

Fig. 1 Schematic view of the composite box-girder with corrugated steel webs

   The corrugated steel webs carry only shear forces, and shear stresses can cause the failure of the webs by shear buckling or yielding, depending on the geometric characteristics of the corrugated steel webs. Also, bending behavior of beams with corrugated steel webs is different from that of conventional beams by nature of the accordion effect and webs eccentrically attached to the flange. Thus, numerous studies have been conducted on the shear buckling of corrugated steel webs (Driver *et al.* 2006, Yi *et al.* 2008, Moon *et al.* 2009) and bending behavior of the composite or I-girder with corrugated steel webs (Elgaaly *et al.* 1997, Machimdamrong *et al.* 2004, Abbas *et al.* 2007, Moon *et al.* 2009). However, only a few studies (Mo *et al.* 2000, Mo and Fan 2006) have been reported regarding the torsional behavior of the composite box-girder bridge with corrugated steel webs, although the torsional behavior is an important design aspect of the bridge superstructure that is subjected to an unbalanced load. Mo *et al.* (2000) proposed an analytical model for torsional behavior of a composite box-girder with corrugated steel webs based on the softened truss model, which was originally developed by Hsu (1988). This softened truss model is known to provide reasonable results for the prediction of the post-cracking behavior and the ultimate strength of concrete structures. However, this model has limitations to predict the entire moment-twist angle relationship including both the pre-cracking and post-cracking response of the composite box-girder with corrugated steel webs, since the softened truss model assumes the section is cracked prior to applying the load and ignores the concrete tension behavior (Chalioris 2006). The concrete tension behavior should be considered for accurate estimation of torsional responses of RC structures as reported by several researchers (Karayannis 2000, Karayannis and Chalioris 2000a, Karayannis and Chalioris 2000b).
   In this study, to overcome the particular disadvantages of the previous analytical model, an improved analytical model for torsion of the composite box-girder with corrugated steel webs considering the concrete tension behavior was developed. The proposed analytical model was verified by comparing with the test and finite element analysis. The proposed model can be capable of predicting the entire torsional moment-twist angle relationship including the initial torsional stiffness, effective torsional stiffness, cracking torsional moment, yielding torsional moment, and ultimate torsional moment. From the results, it was found that the concrete tension behavior has significant effects on the initial stiffness and cracking moment, which are important values by which to evaluate the serviceability of the girder, while it has less significant effect on the ultimate strength of the girder. Finally, a simplified torsional moment-twist angle relationship of the composite box-girder with corrugated steel webs was suggested based on the proposed analytical model for practical engineering purpose.

2. Development of analytical model for torsion of the composite box-girder with corrugated steel webs

2.1 Total torsional moment

The total torsional moment of the composite section consists of torsional moment resisted by upper and lower concrete slabs T_f and torsional moment resisted by corrugated steel webs T_w (Mo *et al.* 2000). Thus, the total torsional moment T can be expressed as

$$T = T_f + T_w \tag{1}$$

It is noted that the Eq. (1) is valid when the corrugated steel webs yield first before the failure of concrete slab. When the concrete failure occurs prior to yielding of corrugated steel web, it leads to the collapse of the whole system and the superposition of torsional moments of each element is no longer applied. In addition, yielding of the corrugated steel webs should occur prior to the failure of concrete slab to guarantee the ductile behavior of the system.

2.2 Pre-cracking behavior

Hsu (1984) reported that the influence of the rebar is of minor importance in the pre-cracking behavior of the reinforced concrete structure, and that the behavior is quite similar with that of the plain concrete structure. Thus, pre-cracking behavior of the slabs of the composite box-girder bridge with corrugated steel webs can be treated as plain concrete. Based on Bredt's thin-walled tube theory (Hsu 1984), the relation among torsional moment T, unit twist angle θ, and shear strain γ can be obtained as

$$T = 2A_o \tau t \qquad \text{(a)}$$
$$\theta = [\, p_o / (2A_o)\,] \gamma \qquad \text{(b)} \tag{2}$$

where A_o is the area enclosed by shear flow; τ is the shear stress; t is the depth of the shear flow; and p_o is the perimeter of the area enclosed by shear flow. Fig. 2 shows the shear flow q that is
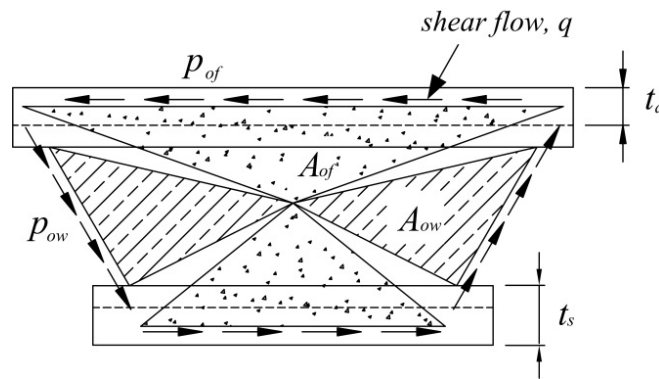

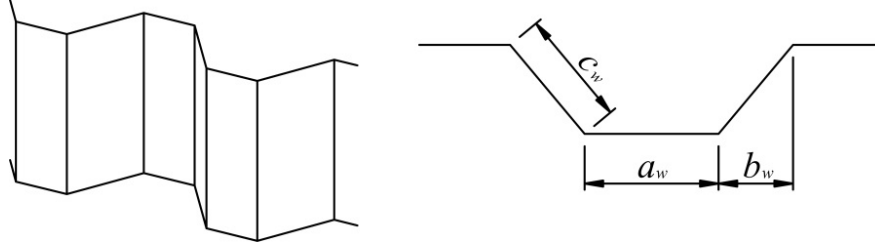Fig. 2 Shear flow on the composite section

Fig. 3 Geometry of the corrugated steel webs

generated along the circumference of the composite section when the pure torsional moment T is applied where A_{ow} and A_{of} are the area enclosed by shear flow in the webs and concrete slabs, respectively; and p_{ow} and p_{of} are the perimeter of the area enclosed by shear flow in the webs and concrete slabs, respectively. In this study, the distortion of the composite section is not considered, and it is assumed that the unit twist angle of the slabs θ_{slab} and the unit twist angle of the webs θ_{web} are the same. Thus, the shear strain of the webs γ_w can be obtained by applying Eq. (2b) to the webs and concrete slabs separately, and γ_w is given by

$$\gamma_w = \frac{A_{ow}}{p_{ow}} \cdot \frac{p_{of}}{A_{of}} \cdot \gamma_f \tag{3}$$

Once the shear strain of the webs γ_w is determined, the shear stress in corrugated steel webs can be obtained by

$$\tau_w = G_{eff}\gamma_w \leq \tau_y \qquad \text{(a)}$$

$$G_{eff} = G\frac{a_w + b_w}{a_w + c_w} \qquad \text{(b)} \tag{4}$$

where τ_y is the yield stress of the webs; τ_w is the shear stress of the webs; and G_{eff} is the effective shear modulus of the corrugated steel webs proposed by Samanta and Mukhopadhyay (1999). The geometry of the corrugated steel webs used in this study is shown Fig. 3. In Eq. (4b), a_w is the flat panel width of the corrugated steel webs; b_w is the horizontal projection of the inclined panel width; c_w is the inclined panel width; and G is the shear modulus of the flat plate.

When the pure torsion is applied to the composite section before cracking, shear stress in the concrete slab τ_f has the same value with the principal tensile stress, and the relationship of $G_c\gamma_f = E_c\varepsilon_r$ is satisfied, where E_c and G_c are the elastic and shear modulus of the concrete; and ε_r is the principal tensile strain of the concrete slabs. Thus, by using Eq. (2a), torsional moment resisted by upper and lower concrete slabs T_f and torsional moment resisted by corrugated steel webs T_w can be expressed as

$$T_f = 2A_{of}t_s\tau_f = 2A_{of}t_sE_c\varepsilon_r \qquad \text{(a)}$$

$$T_w = 2A_{ow}t_w\tau_w \qquad \text{(b)} \tag{5}$$

where t_s and t_w are the thicknesses of the slabs and the webs, respectively. Finally, the total
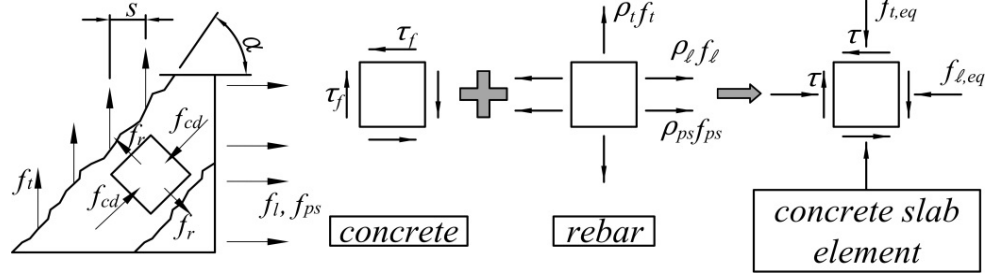
Fig. 4 Stresses in concrete slab

torsional moment resistance before the cracking of the composite box-girder with corrugated steel webs can be obtained by Eq. (1) with Eqs. (3)-(5) for a given principal tensile strain of the concrete slabs.

2.3 Post-cracking behavior

2.3.1 Equilibrium equation

Fig. 4 shows the relationship of the stress in the slabs after the concrete is cracked. In Fig. 4, subscripts *l*, *t*, and *ps* represent the longitudinal rebar, transversal rebar, and pre-stressing tendon, respectively. In this study, the equilibrium equation of the concrete slabs is derived by using a smeared truss model (Hsu 1984). This model assumes that the tensile stress in the rebar and pre-stressing tendon act on the concrete as equivalent compressive stresses as shown in Fig. 4. By applying the force equilibrium condition, equivalent longitudinal stress $f_{l,eq}$ and equivalent transversal stresses $f_{t,eq}$ are obtained as

$$f_{l,eq} = \frac{A_l f_l + A_{ps} f_{ps}}{p_{of} t_d} \qquad \text{(a)}$$

$$\tag{6}$$

$$f_{t,eq} = \frac{A_t f_t}{s t_d} \qquad \text{(b)}$$

where *A* is the area; *s* is the spacing of the transversal rebar; and t_d is the effective depth of the shear flow. By using Mohr's circle for the stress and assuming that the angle of principal axis is the same as cracking angle, α, $f_{l,eq}$, and $f_{t,eq}$ can be expressed as the following equations in terms of principal stresses and cracking angle α

$$f_{l,eq} = f_{cd} cos^2\alpha - f_r sin^2\alpha \qquad \text{(a)}$$

$$f_{t,eq} = f_{cd} sin^2\alpha - f_r cos^2\alpha \qquad \text{(b)} \qquad (7)$$

$$\tau_f = (f_{cd} + f_r) sin\alpha \, cos\alpha \qquad \text{(c)}$$

In Eq. (7), f_{cd} and f_r are the principal compressive stress and tensile stress, respectively. By rearranging Eq. (6) and (7), the effective depth of the shear flow t_d and cracking angle α can be obtained as

$$t_d = \frac{1}{f_{cd} - f_r}\left(\frac{A_l f_l + A_{ps} f_{ps}}{p_{of}} + \frac{A_t f_t}{s}\right) \quad \text{(a)}$$

$$\cos\alpha = \frac{1}{f_{cd} + f_r}\frac{1}{t_d}\left(\frac{A_l f_l + A_{ps} f_{ps}}{p_{of}} - \frac{A_t f_t}{s}\right) \quad \text{(b)}$$

(8)

Then, torsional moment resisted by upper and lower concrete slabs T_f can be calculated by substituting Eq. (7) into Eq. (2) with the effective depth of the shear flow t_d described in Eq. (8), and T_f is given by

$$T_f = 2A_{of} t_d \tau_f = A_{of} t_d (f_{cd} + f_r)\sin 2\alpha \tag{9}$$

In the case of the torsional moment resisted by corrugated steel webs T_w, Eq (5b) is still applicable regardless of the appearance of the cracking on the concrete slab.

2.3.2 Compatibility equation
Fig. 5 shows the strain distribution in the concrete strut. Compressive and tensile strain is assumed to be linearly varied from the bottom to the top of the concrete slabs as shown in Fig. 5. When the effective depth of the shear flow t_d is smaller than the thickness of the slabs t_s, the principal compressive strain ε_d and the principal tensile strain ε_r are half of the maximum compressive strain ε_{ds} and the maximum tensile strain ε_{rs}, respectively. When t_d is the same as t_s, ε_d
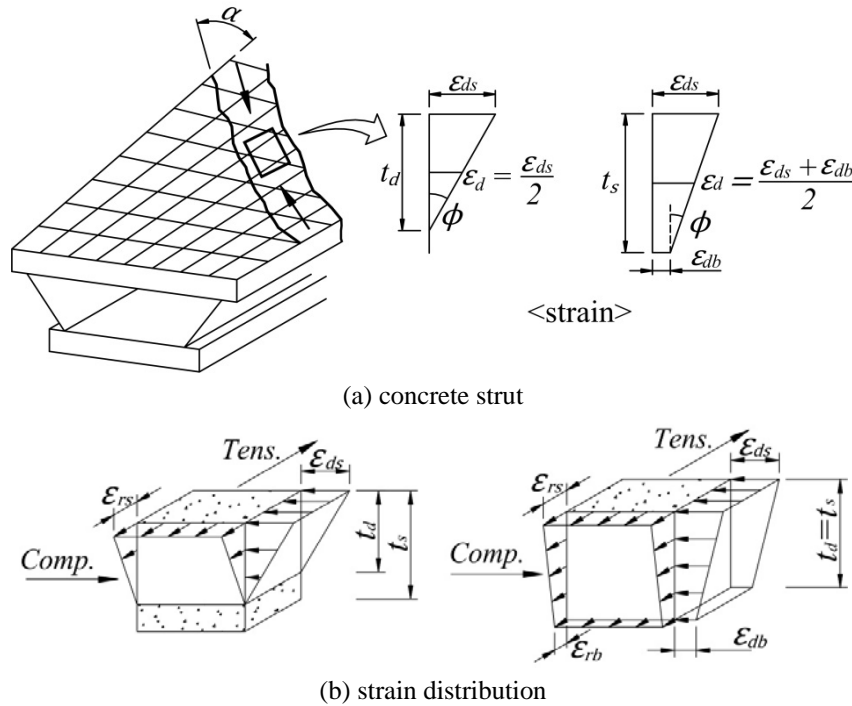

(a) concrete strut

(b) strain distribution

Fig. 5 Stress and strain distribution in concrete strut

(a) distortion due to ε_l (b) distortion due to ε_t (c) distortion due to ε_d
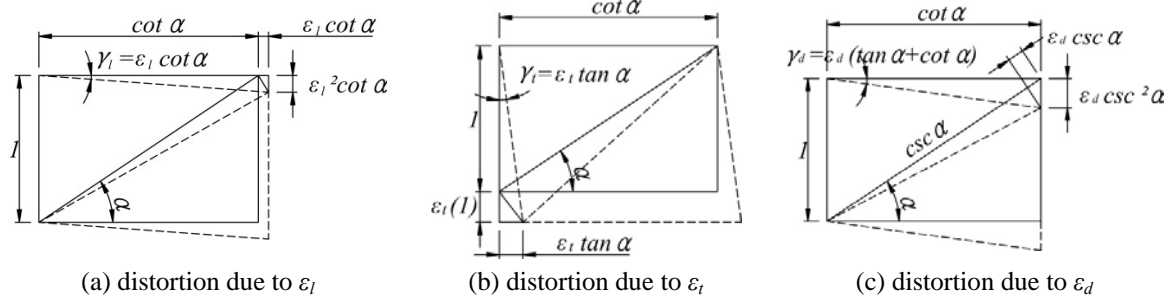
Fig. 6 Geometrical relationship of strains

and ε_r are defined as the average value of the maximum and minimum strain on the top and bottom surface as shown in Fig. 5(b). From the compressive strain distribution of the concrete strut, the curvature of the concrete strut ϕ is defined as $(\varepsilon_{ds} - \varepsilon_{db}) / t_d$, as shown in Fig. 5(a). The relationship between the unit twist angle θ and the curvature of the concrete strut ϕ is given by $\phi = \theta \sin 2\alpha$ (Hsu 1984). Combining theses equations and substituting them into Eq. (2b), θ and γ_f can be expressed in terms of ε_{ds} and ε_{db} as follows

$$\theta = \frac{\varepsilon_{ds} - \varepsilon_{db}}{2t_d \sin\alpha \cos\alpha} \qquad \text{(a)}$$

$$\gamma_f = \frac{2A_{of}}{p_{of}} \frac{\varepsilon_{ds} - \varepsilon_{db}}{2t_d \sin\alpha \cos\alpha} \qquad \text{(b)}$$

(10)

Figs. 6(a)-(c) show the geometrical relationship of strain (Hsu 1984). In Figs. 6(a)-(c), ε_l is the longitudinal rebar strain; and ε_t is the transversal rebar strain. The shear strain of the concrete slab γ_f is obtained by summing the individual strain and is given by

$$\gamma_f = \gamma_l + \gamma_t + \gamma_d = (\varepsilon_l + \varepsilon_d)\cot\alpha + (\varepsilon_t + \varepsilon_d)\tan\alpha \qquad (11)$$

Substituting Eq. (10b) into Eq. (11) with the relationship of $\tan^2\alpha = (\varepsilon_d + \varepsilon_l)/(\varepsilon_d + \varepsilon_t)$, which is the condition that γ_f has the minimum value, the longitudinal and transversal strains of the rebar are derived as

$$\varepsilon_t = \frac{A_{of}(\varepsilon_{ds} - \varepsilon_{db})}{2t_d p_{of} \sin^2\alpha} - \frac{\varepsilon_{ds} + \varepsilon_{db}}{2} \qquad \text{(a)}$$

$$\varepsilon_l = \frac{A_{of}(\varepsilon_{ds} - \varepsilon_{db})}{2t_d p_{of} \cos^2\alpha} - \frac{\varepsilon_{ds} + \varepsilon_{db}}{2} \qquad \text{(b)}$$

(12)

For the pre-stressing tendon, the strain of the pre-stressing tendon ε_{ps} is given by (Mo *et al.* 2000)

$$\varepsilon_{ps} = \varepsilon_{pi} + \varepsilon_{li} + \varepsilon_l \qquad (13)$$

in which

$$\varepsilon_{pi} = f_{pi}/E_p \qquad (a)$$

$$\varepsilon_{li} = \frac{A_{ps}f_{pi}}{A_l E_s + (A_c - A_{ps} - A_l - A_{t,eq})E_c} \qquad (b) \tag{14}$$

In Eq. (14), ε_{pi} is initial strain of pre-stressing tendon; ε_{li} is the initial strain of longitudinal rebar; f_{pi} is the initial tensile stress; E_p is the elastic modulus of the pre-stressing tendon; E_s is the elastic modulus of the steel; A_c is the area of the slabs; and $A_{t,eq}$ is the equivalent area of the transversal rebar, which is the volume per unit length along with longitudinal direction. Finally, the relation between each strain of the concrete slab can be expressed by using Mohr's strain circle and given by (Hsu 1984)

$$\varepsilon_r = \varepsilon_l + \varepsilon_t + \varepsilon_d \tag{15}$$

2.3.3 Stress-strain relationship

The compressive strength of the concrete is reduced when the concrete is subjected to bi-axial stress loading. To take account of this phenomenon, Belarbi and Hsu (1995) proposed the softened concrete model, and their constitutive model is adopted in this study. The softened concrete model proposed by Belarbi and Hsu (1995) is described in Fig. 7, and mathematical expression is given by

$$\varepsilon_c \le \beta\varepsilon_o, \; f_c = f_c'\left[2\left(\frac{\varepsilon_c}{\beta\varepsilon_o}\right) - \left(\frac{\varepsilon_c}{\beta\varepsilon_o}\right)^2\right] \qquad (a)$$

$$\varepsilon_c > \beta\varepsilon_o, \; f_c = f_c'\left[1 - \left(\frac{\dfrac{\varepsilon_c}{\beta\varepsilon_o} - 1}{\dfrac{2}{\beta} - 1}\right)^2\right] \qquad (b) \tag{16}$$

where ε_c is compressive strain of the concrete; ε_o is peak strain of the concrete; f_c is compressive stress of the concrete; f_c' is the uni-axial compressive strength of the concrete; and β is the softening coefficient and is defined by (Mo *et al.* 2000)

$$\beta = \frac{0.9}{\sqrt{1 + 600\varepsilon_r}} \tag{17}$$

For the tension of the concrete, it is assumed that the tensile stress is linearly increased with increasing tensile strain before cracking. After the cracking, the tension stiffening effect is considered. In this study, the tension stiffening model proposed by Vecchio and Collins was adopted for the analysis and it is given by (Collins and Mitchell 1991)
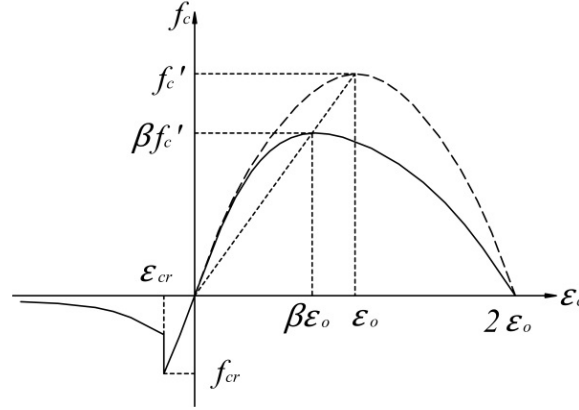
Fig. 7 Stress-strain relationship of softened concrete

$$\varepsilon_{ct} \leq \varepsilon_{cr}, \; f_c = E_c \varepsilon_{ct} \qquad (a)$$

$$\varepsilon_{ct} > \varepsilon_{cr}, \; f_c = \frac{f_{cr}}{1 + \sqrt{500\varepsilon_{ct}}} \qquad (b) \qquad\qquad (18)$$

where ε_{ct} is tensile strain of the concrete; ε_{cr} is cracking strain of the concrete; and f_{cr} is the cracking stress of the concrete.

For the corrugated steel webs, the elastic-perfectly plastic stress-strain relationship was used. Eq. (4) is valid up to τ_y, and shear stress in the corrugated steel webs is the same as τ_y after the web has yielded.

2.4 Analysis procedure

Fig. 8 shows the iterative analysis procedure for torsion of the composite box-girder with corrugated steel webs. In this analysis, the main parameter was maximum compressive strain ε_{ds}. The analysis was conducted by increasing ε_{ds} with increments of 10^{-5} up to 0.0035. Pre-cracking formulation described in Section 2.2 was applied when the maximum tensile strain on the top surface ε_{rs} is smaller than the cracking strain of the concrete ε_{cr}. If ε_{rs} is larger than ε_{cr}, post-cracking formulation in Section 2.3 is used for the analysis. For the calculation of post-cracking behavior, cracking angle α, effective depth of the shear flow t_d, and maximum tensile strain ε_{rs} are assumed for given ε_{ds}. Minimum compressive strain ε_{db} and minimum tensile strain ε_{rb} are also assumed as zero first. The strain of the rebar, and pre-stressing tendon were calculated from Eqs. (12)-(14). Corresponding stresses were then obtained by using the constitutive law presented in Section 2.3.3. By using Eq. (8) and (15), the assumed α, t_d, and ε_r were re-calculated, and the values were compared with the initially assumed ones. Iteration was then repeated until the difference between the assumed and re-calculated values is smaller than the convergence criteria shown in Table 1. Once the assumed α, t_d, and ε_r satisfy the convergence criteria, T_f and T_w were determined by Eq. (9) and Eq. (5b), respectively. By repeating the above procedure, the whole relationship between T and θ can be obtained.
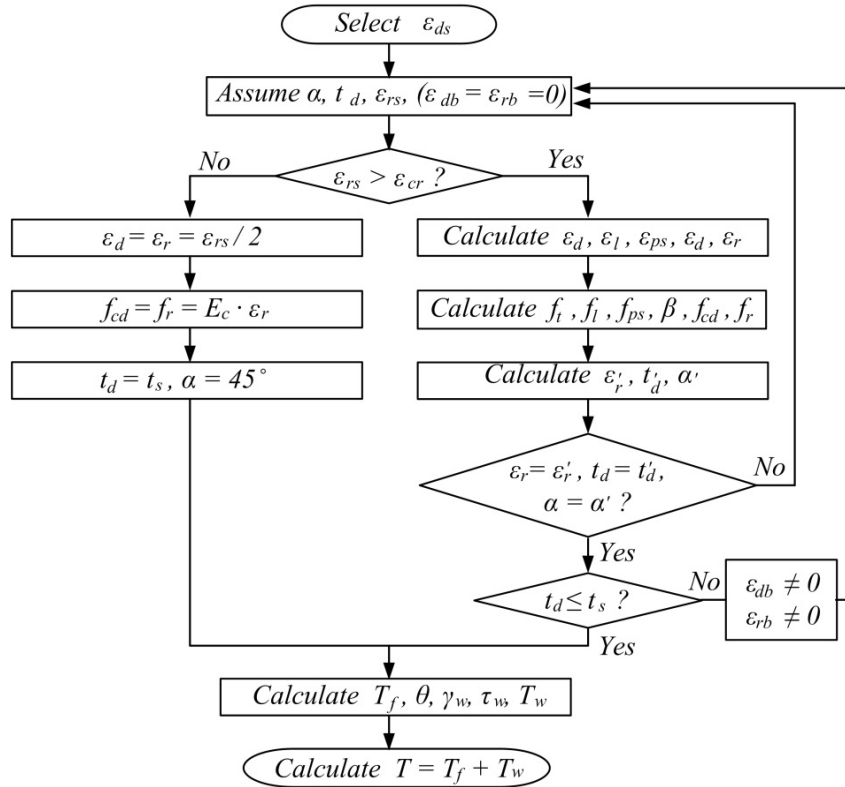
Fig. 8 Flowchart for torsional analysis of composite girder with corrugated steel webs

Table 1 Convergence criteria

Variable	Equation	Convergence criteria
ε_r	Eq. (15)	10^{-9}
t_d	Eq. (8a)	10^{-6}
α	Eq. (8b)	10^{-9}

3. Verification of the proposed analytical model

3.1 Test specimen and setup

A test on the torsion of the composite box-girder with corrugated steel webs was conducted, and the results were compared with the proposed analytical model for verification purposes. The dimensions of the test specimen are shown in Fig. 9(a). The thickness of the corrugated steel webs was 4 mm; the flat panel width of the corrugated steel webs a_w was 80 mm; the horizontal projection of the inclined panel width b_w was 80 mm; and the inclined panel width c_w was 100 mm. The height of the corrugated steel webs was 350 mm, and the concrete slabs having a 150 mm thickness was attached at the top and bottom of the corrugated steel webs. Fig. 9(b) shows the profiles of the rebar where the diameter of the rebar was 16 mm. From the material test, the

compressive strength of the concrete, the yield stress of the steel, and ultimate stress of the steel were 40, 255, and 400 MPa, respectively. The length of the specimen is 1,800 mm, and concrete blocks were attached at the ends of the specimen to provide the space for boundary and loading as shown in Fig. 9(a). The test setup is shown in Figs. 10-11. The left concrete block was fixed at the strong floor of the laboratory, and the load was applied to the right concrete block as shown in Fig. 11. The strong steel bar was inserted into the anchor hole in the right concrete block to prevent the in-plane deflection, but it was free to rotate. Two linear variable displacement transducers (LVDT) were placed to measure vertical deflection and calculate the rotation of the specimen as shown in Fig. 11.

(a) dimension of the specimen
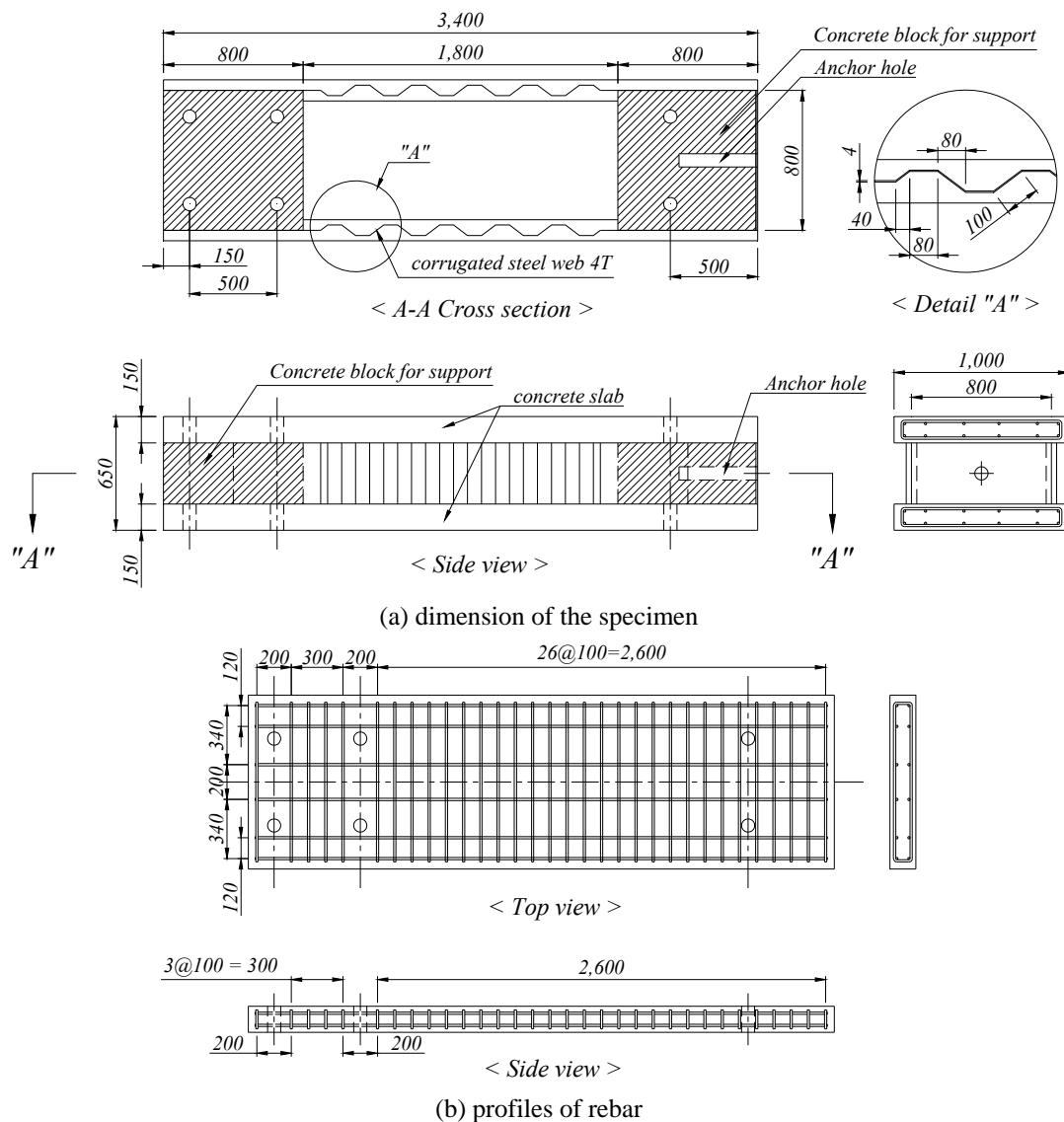
(b) profiles of rebar
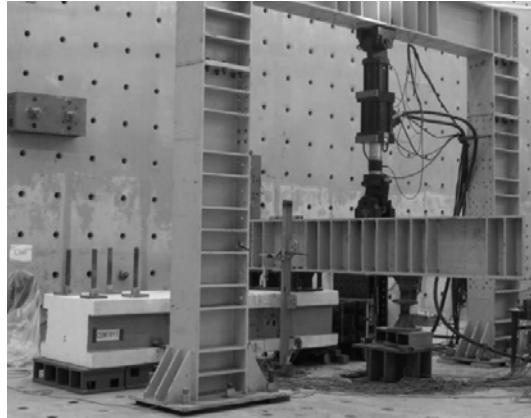
Fig. 9 Test specimen (unit: mm)
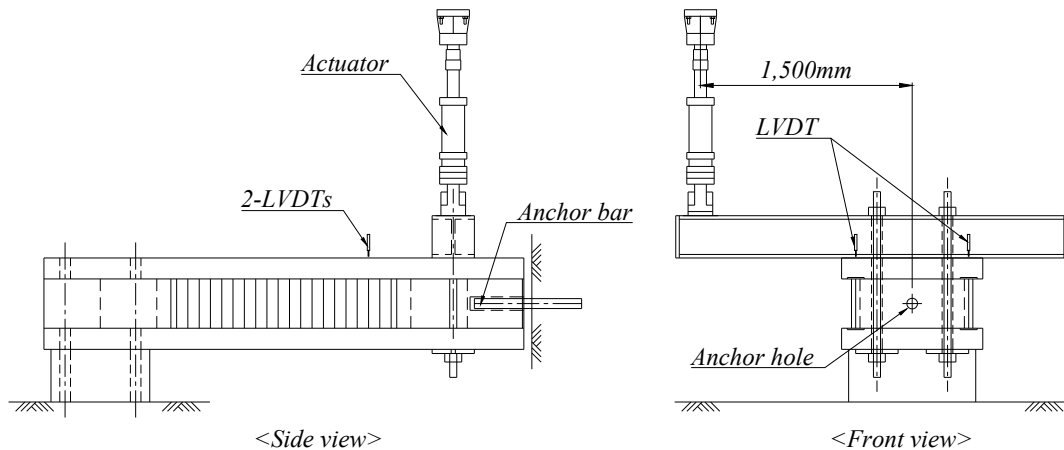
Fig. 10 Photo of test setup

Fig. 11 Test setup and data acquisition system

3.2 Finite element analysis model

Finite element analysis was conducted for additional verification of the proposed analytical model for the torsion of the composite box-girder with corrugated steel webs. The general purpose structural analysis program ABAQUS (2010) was used for the analysis. Fig. 12 shows the finite element model for the test specimen. An 8-node solid element (C3D8R) and a 4-node shell element (S4R) were used to model the concrete slab and corrugated steel webs, respectively. A non-linear spring element was used to model the stud in the interface between the concrete slabs and the corrugated steel webs. The mathematical load-slip relationship of stud proposed by Shima and Watanabe (2009) was adopted for modeling of the non-liner spring element in the interface. To apply the torsional moment to the analysis model, all nodes in the left end were connected to the geometric center of the section by a 2-node 3-dimensional rigid beam element (RB3D2) as shown in Fig. 12. The torsional moment was then applied to the geometric center where rotations about X, Y directions and displacements in X, Y, Z directions were restrained. All degree of freedom of the right end of the finite element model were restrained to provide the fixed end.
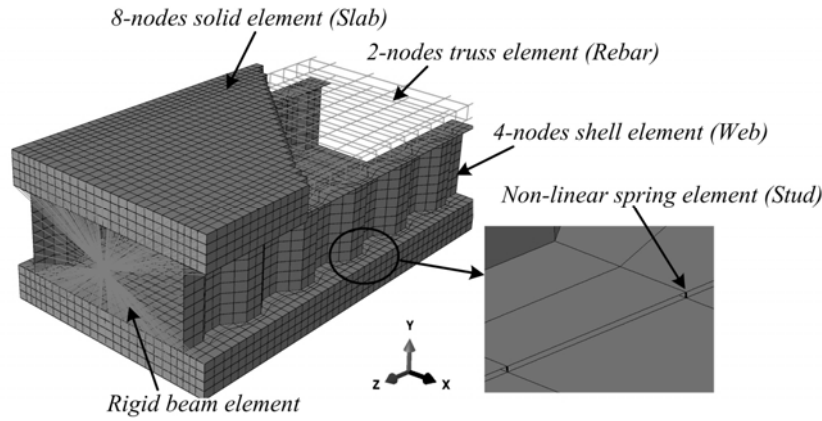
Fig. 12 Finite element model for test specimen

The concrete damaged plasticity model in ABAQUS (2010) was employed to simulate the non-linear behavior of the concrete. This model follows the non-associated flow rule, and flow potential is a function of dilation angle ψ. The dilation angle of the concrete varies significantly depending on the concrete properties. In this study, ψ of 45° was adopted for the analysis based on the results of parametric study.

The stress-strain relationship of the concrete under uni-axial compression was modeled with general parabolic curve as

$$f_c = f_c' \left[2\left(\frac{\varepsilon_c}{\varepsilon_0} \right) - \left(\frac{\varepsilon_c}{\varepsilon_0} \right)^2 \right] \qquad (19)$$

where it is assumed that the stress-strain relationship is linear up to a stress of 0.5 f_c'. The linear behavior of the concrete E_c was approximated as the following equation (ACI 2008)

$$E_c = 4{,}730\sqrt{f_c'} \ \ (MPa) \qquad (20)$$

For the case of the tension behavior of the concrete, tension stiffening model proposed by Vecchio and Collins was employed (Collins and Mitchell 1991). For the steel, the Von-Mises yield criterion with isotropic hardening rule was adopted, and the measured stress-stain relationship was used for the analysis.

3.3 Comparison with proposed analytical model

Fig. 13 shows the comparison of the T-θ relationship with test results and finite element analysis. The test was terminated when θ was approximately 0.20 rad/m because of the failure of the concrete near the loading region. However, the stiffness of the T-θ relationship of the test specimen was almost zero when the test was terminated, and the strength at this point was determined as the ultimate strength of the test specimen. From the test, the initial torsional stiffness K and the ultimate torsional moment T_u were 2.485×10^5 kN·m² and 679.04 kN·m,

(a) $f_{cr} = 7.5\%$ of f_c'
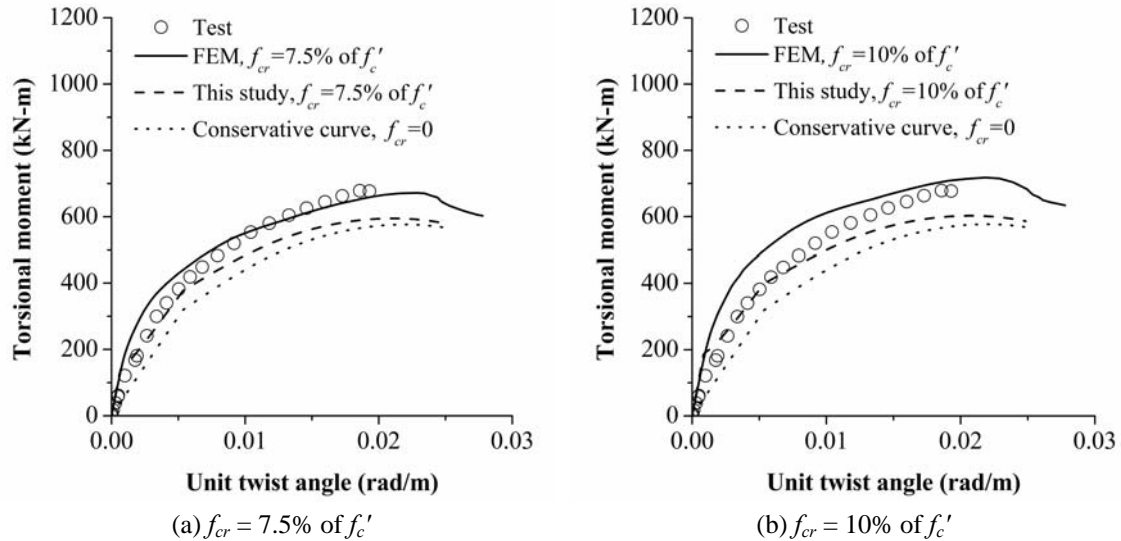
(b) $f_{cr} = 10\%$ of f_c'

Fig. 13 Comparison of the torsion-twist angle relationship with test results and finite element analysis

respectively.

The analysis was conducted for the various values of the tensile strength of the concrete ($f_{cr} = 0.075$, and $0.1 f_c'$) to evaluate its effect on the torsional behavior of box-girder bridge with corrugated steel webs because the tensile strength of the concrete varies depending on the concrete properties. The dashed line and solid line in Fig. 13 represent the results of the proposed analytical model and finite element analysis, respectively. Also, the dotted line in Fig. 13 shows the results of the proposed analytical model when f_{cr} is equal to zero.

For the various values of f_{cr}, a comparison of the initial torsional stiffness K and ultimate torsional moment T_u with test results are shown in Table 2. From the results, initial torsional stiffness obtained from the proposed analytical model and finite element model were 2.22×10^5 and 2.06×10^5 kN·m^2, respectively and the initial torsional stiffness has the same value regardless of the tensile strength of the concrete except where $f_{cr} = 0$. The proposed analytical model and finite element analysis underestimated the initial torsional stiffness by 12 and 21%, respectively as shown in Table 2. In the case of ultimate torsional moment T_u, the proposed analytical model underestimated the ultimate torsional moment by around 13%; while the finite element analysis provided better estimation of the ultimate torsional moment (The average discrepancy is 2.2%). When the concrete tension behavior is not considered ($f_{cr} = 0$), the proposed analytical model

Table 2 Comparison of initial torsional stiffness and ultimate strength with test results

Case	K from test (kN·m^2)	Test/ proposed	Test/ FEM	T_u from Test (kN·m)	Test/ proposed	Test/ FEM
$f_{cr} = 7.5\%$ of f_c'	2.485×10^5	1.12	1.21	679.04	1.14	1.01
$f_{cr} = 10\%$ of f_c'		1.12	1.21		1.13	0.95

underestimates the initial stiffness and ultimate strength of the test specimen by 75.6 and 15.1%, respectively. Thus, it shows that the effect of the concrete tension behavior on the initial stiffness is significant, and it should be considered in the analysis. From the results of comparative study, the analysis model with $f_{cr} = 0.075 f_c'$ provided a good comparison with the test results for both the proposed analytical model and finite element analysis.

Fig. 14 shows the comparison of the crack pattern of the concrete slab. The cracking angle was approximately 44.5° and 43.5° from the test and finite element analysis, respectively, and these values are almost identical with 46.4°, which is the result from the proposed analytical model.

A further verification was performed using the test results of the other researchers (Mo *et al*. 2000). Fig. 15 shows the comparison of the *T-θ* relationship with analytical results and test results (Mo *et al*., 2000). Generally, the analysis results with $f_{cr} = 0$ (dotted line) showed a little bit more conservative results than those with the effect of tensile behavior of the concrete (solid line). The
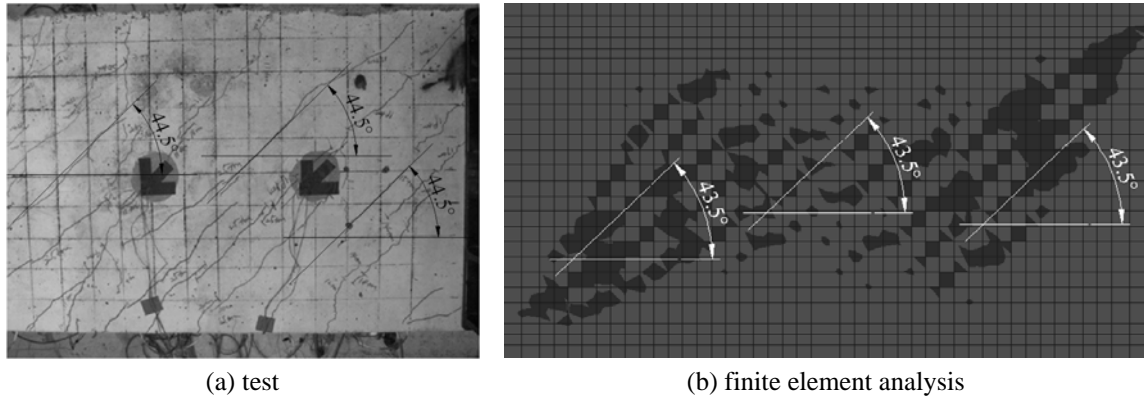

| (a) test | (b) finite element analysis |

Fig. 14 Comparison of crack pattern
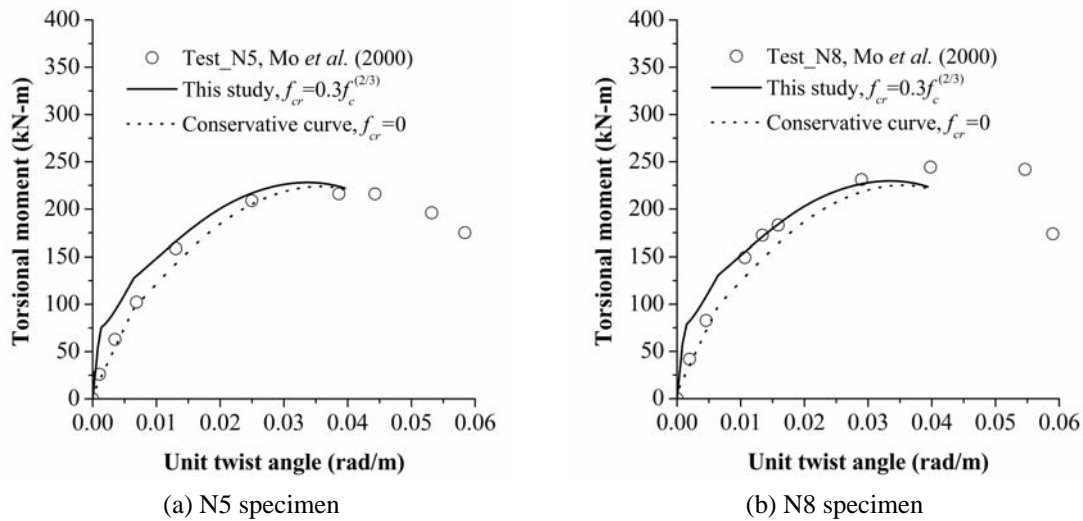

| (a) N5 specimen | (b) N8 specimen |

Fig. 15 Comparison of the torsion-twist angle relationship with analytical model and test results by Mo *et al*. (2000)

later model gave more accurate prediction of the torsional behavior in inelastic region while it overestimated the initial stiffness, as shown in Fig. 15. It should be noted that the tensile strength of the concrete f_{cr} is assumed as $0.3 f_c'^{(2/3)}$ based on the EC-2 (2004). However, f_{cr} used in this study may not be proper for the case of Mo *et al.* (2000) since f_{cr} was not reported in their study.

4. Simplified *T-θ* relationship for composite box-girder bridge with corrugated steel webs

4.1 Proposed simplified T-θ relationship

A simplified T-θ relationship for the composite box-girder with corrugated steel webs was proposed based on the available current design code and proposed analytical model for the practical engineering purpose herein. Fig. 16 shows the schematic view of the simplified T-θ relationship of the composite box-girder with corrugated steel webs. Three different stiffness were suggested in this study. K represents the initial stiffness prior to cracking torsional moment T_{cr}; K_{eff} denotes the stiffness that can be measured from the origin *o* to the yielding torsional moment T_y that is defined as the moment corresponding to the yielding of the corrugated steel webs; and K_{cr} indicates the stiffness after corrugated steel webs have yielded. Thus, the whole T-θ relationship of the composite box-girder with corrugated steel webs can be constructed by connecting *o*, *A*, *B*, *C*, and *D* as shown in Fig. 16. Based on the developed analysis program and available current design code, K, K_{eff}, T_{cr}, T_y, and T_u were proposed through following Section 4.2–4.4.

4.2 Stiffness of the composite box-girder bridge with corrugated steel webs

In this study, initial torsional stiffness K was derived based on the pre-cracking formulation described in Section 2.2, and the proposed K is given by

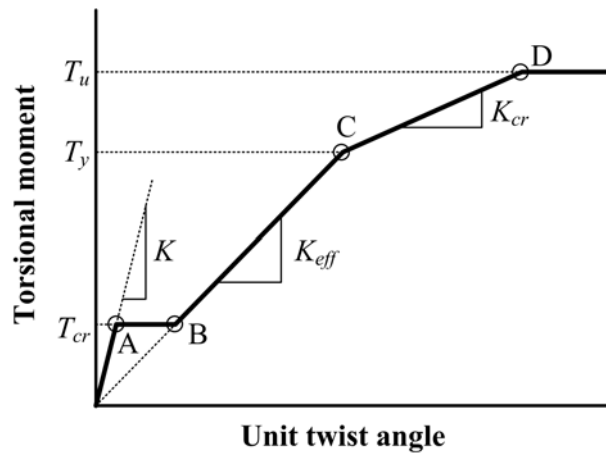$$K = G_c \frac{4A_{of}^2 t_s}{p_{of}} + G_{eff} \frac{4A_{ow}^2 t_w}{p_{ow}} \tag{21}$$

Fig. 16 Schematic view of simplified *T-θ* relationship

In Eq. (21), the left and right parts of the equation represent the torsional stiffness of the concrete slab and the corrugated steel webs, respectively. This initial torsional stiffness is reduced to K_{eff} after cracking occurs in the concrete slab. Hsu (1984) proposed post-cracking shear modulus G_{cr} for the reinforced concrete structures, and K_{eff} can be simply obtained by substituting G_{cr} into the left part of Eq. (21). Thus, K_{eff} can be expressed as

$$K_{eff} = \frac{E_r}{\left(4n_r + \dfrac{1}{\rho_l} + \dfrac{1}{\rho_t} \right)} \frac{4A_{of}^2 t_s}{p_{of}} + G_{eff} \frac{4A_{ow}^2 t_w}{p_{ow}} \tag{22}$$

where E_r is the elastic modulus of rebar; n_r is E_r / E_c; ρ_l is the longitudinal reinforcement ratio; and ρ_t is the transversal reinforcement ratio. Once corrugated steel webs have yielded, the torsional stiffness of the corrugated steel webs becomes zero. Thus, K_{eff} is reduced to K_{cr}, and K_{cr} can be obtained assuming the right part of the Eq. (22) is equal to zero.

4.3 Cracking and yielding moment of composite box-girder bridge with corrugated steel webs

In this section, cracking and yielding torsional moment are derived based on the proposed analytical model. It is noted that cracking torsional moment T_{cr} is defined as torsional moment that generates cracking on the concrete surface. Thus, the condition of $\varepsilon_r = \varepsilon_{rs}/2 = \varepsilon_{cr}/2$ is satisfied by using this condition with Eqs. (1)-(5) in Section 2. T_{cr} can be expressed as

$$T_{cr} = A_{of} E_c \varepsilon_{cr} \left\{ t_s + n_s t_w \frac{p_{of}}{p_{ow}} \left(\frac{A_{ow}}{A_{of}} \right)^2 \right\} \tag{23}$$

Yielding torsional moment T_y is the torsional moment that corresponding to the yielding of corrugated steel webs. Thus, shear strain of the webs γ_w is equal to γ_y. Applying this condition with the compatibility condition in Eq. (3), the shear strain of the concrete slab γ_f at T_y can be calculated. Then, the shear stress of the concrete slab τ_f can be obtained as $G_{cr}\gamma_f$. By using this shear stress of the concrete slab with Eq. (1), (5b), and (9), the yielding torsional moment T_y can be obtained as

$$T_y = 2G_{cr} \frac{p_{ow}}{A_{ow}} \frac{\gamma_y}{p_{of}} A_{of}^2 t_d + 2A_{ow} t_w \tau_y \tag{24}$$

Eq. (24) is a function of t_d, and it is hard to predict t_d at T_y without the iteration procedure described in Section 2.4. For the simplicity of the calculation, t_d is assumed to be same as t_s, in this study, and this assumption was verified with the case study in Section 4.5.

4.4 Ultimate torsional moment of the composite box-girder bridge with corrugated steel webs

The equation to estimate the ultimate torsional moment of the composite box-girder with corrugated steel webs was derived based on the ACI design specification herein. ACI (2008)

suggests ultimate torsional moment for reinforced concrete structure as

$$T_u = \frac{2A_o A_t f_{ty}}{s} \cot \alpha \tag{25}$$

where f_{ty} is the yield stress of transversal rebar. Eq. (25) was derived neglecting the strength of the concrete and assuming that the transverse rebar is yielded at the ultimate state. To assure that the transverse rebar has yielded first before the yielding of the longitudinal rebar, the total area of the longitudinal rebar has to be larger than

$$A_l = \frac{A_t}{s} p_o \left(\frac{f_{ty}}{f_{ly}} \right) \cot^2 \alpha \tag{26}$$

where f_{ly} is the yield stress of the longitudinal rebar.

The ultimate torsional moment of the composite box-girder with corrugated steel webs consists of torsional moment resisted by upper and lower concrete slabs T_f and torsional moment resisted by corrugated steel webs T_w as described in Eq. (1). Thus, assuming corrugated steel webs and transversal rebar have yielded at the ultimate state, the ultimate torsional moment of the composite box-girder with corrugated steel webs can be expressed as

$$T_u = \frac{2A_{of} A_t f_{ty}}{s} \cot \alpha + 2A_{ow} t_w \tau_y \tag{27}$$

4.5 Verification of the proposed simplified T-θ relationship

The simplified *T-θ* relationship proposed in this study was verified by comparing the results of the proposed analytical model and finite element analysis. For the comparison, four different composite box-girders with corrugated steel webs were analyzed, and the detail dimensions of the analysis models are shown in Table 3. Case 1 and 2 have the same geometry except for the reinforcement ratio in the concrete slab, and Case 3 and 4 have different thicknesses of concrete slabs, but other properties are identical each other as shown in Table 3. From the results, the simplified model generally provided more conservative results than the proposed analytical model and finite element analysis as shown in Fig. 17 and Table 4. The initial torsional stiffness from the simplified model were exactly the same as those of the proposed analytical model, while the simplified model underestimated the ultimate strength T_u by 5.3% comparing to the proposed analytical model. This is because the effect of concrete strength is not considered in Eq. (27). The average discrepancy of K_{eff} and T_y between the simplified and the proposed analytical model were 13.8 and 13%, respectively. A comparatively large discrepancy was observed in cracking torsional moment T_{cr}. In the proposed analytical model and finite element analysis, the stiffness reduction is initiated after the first crack on the concrete surface is formed, and the stiffness is gradually decreased. However, in the simplified model, stiffness is suddenly changed at T_{cr} from K to K_{eff}, and this results in a conservative prediction of deformation in the inelastic region as shown in Fig. 17. However, the simplified model provided reasonable overall behavior of the composite box-girder with corrugated steel webs under pure torsion.
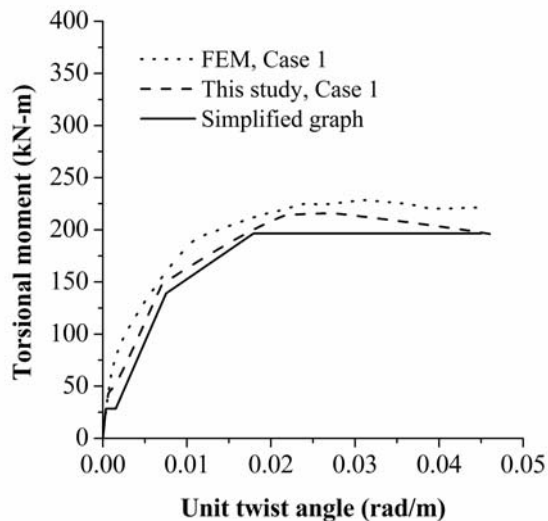
Table 3 Profiles of analysis models

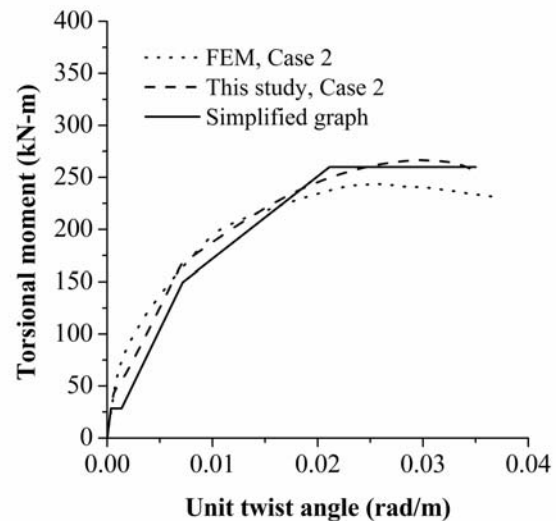| Model	Web (mm)			Slab (mm)	Reinforcement ratio	
	Width	Height	Thickness	Thickness	Longitudinal	Transversal
Case 1	600	350	3	90	0.014	0.011
Case 2	600	350	3	90	0.020	0.018
Case 3	1600	875	7	300	0.015	0.015
Case 4	1600	875	7	360	0.013	0.013
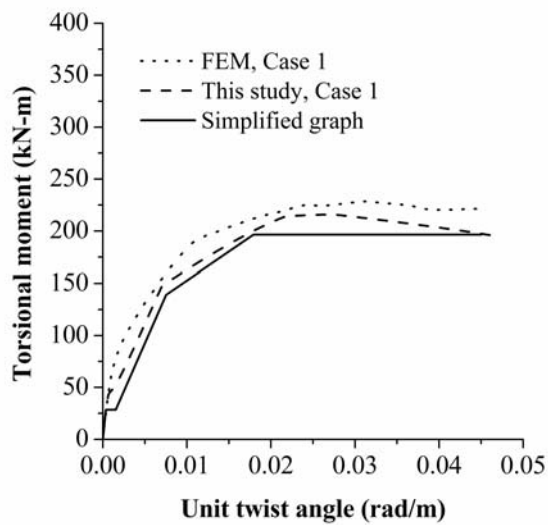
(a) Case 1
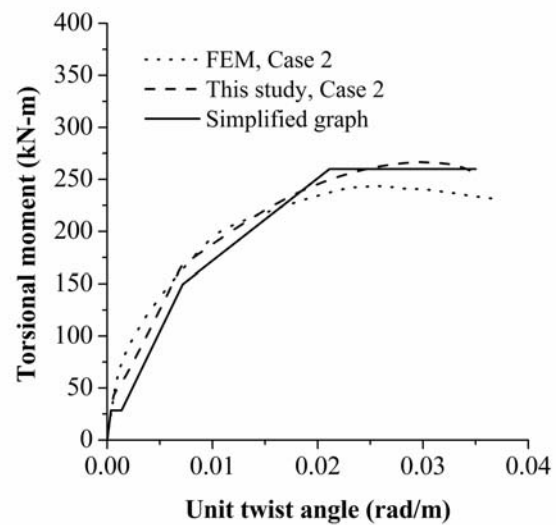
(b) Case 2

(c) Case 3

(d) Case 4

Fig. 17 Comparison of simplified T-θ relationship with analytical model and finite element analysis

Table 4 Comparison of simplified graph with the results of analysis

	Case 1	Case 2	Case 3	Case 4
	Simplified/proposed	Simplified/proposed	Simplified/proposed	Simplified/proposed
K	1.0	1.0	1.0	1.0
T_{cr}	0.67	0.66	0.71	0.76
K_{eff}	0.88	0.88	0.86	0.83
T_y	0.94	0.90	0.84	0.80
T_u	0.91	0.97	0.98	0.93

5. Conclusions

In this study, an improved non-linear analytical model for torsion of the composite box-girder with corrugated steel webs considering the concrete tension behavior was developed. The proposed model is capable of predicting the entire torsional moment-twist angle relationship including initial torsional stiffness, effective torsional stiffness, cracking torsional moment, yielding torsional moment, and ultimate torsional moment, and the model was verified by comparing with the results of tests and finite element analysis. From the verification results, it is found that the effect of the concrete tension behavior on the initial stiffness is significant, and it should be considered in the analysis, while the effect of concrete tension behavior on the ultimate strength is less significant. The magnitude of the concrete tensile strength is directly proportional to cracking torsional moment, but it doesn't affect to initial torsional stiffness.

For practical engineering purposes, a simplified T-θ relationship was proposed based on the current design specification and developed analytical model. The proposed simplified T-θ relationship was then verified by comparing it with the proposed analytical model and finite element analysis. From the comparative study, it can be seen that the simplified model provided reasonable overall behavior of the composite box-girder with corrugated steel webs under pure torsion.

Acknowledgements

References

ABAQUS (2010), *Abaqus Analysis User's Manual version 6.10.*, Dassault Systèmes Simulia Corp.

Abbas, H.H., Sause, R. and Driver R.G. (2007), "Analysis of flange transverse bending of corrugated web I-girders under in-plane loads", *ASCE J. Struct. Eng.*, **133**(3), 347-355.

ACI (2008), *Building Code Requirements for Structural Concrete and Commentary*, ACI 318M-08 American Concrete Institute, Detroit, MI.

Belarbi, A. and Hsu, T.T.C. (1995), "Constitutive laws of softened concrete in biaxial tension-compression", *ACI Struct. J.*, **92**(5), 562-573.

CEN (2004), *Eurocode 2: Design of Concrete Structures: Part 1-1: General Rules and Rules for Buildings*, Brussels.

Chalioris, C.E. (2006), "Experimental study of the torsion of reinforced concrete members", *Struct. Eng. Mech.*, **23**(6), 713-737.

Collins, M.P. and Mitchell, D. (1991), *Prestressed concrete structures*, Prentice-Hall, Englewood Cliffs, NJ.

Driver, R.G., Abbas, H.H. and Sause, R. (2006), "Shear behavior of corrugated web bridge girder", *ASCE J. Struct. Eng.*, **132**(2), 195-203.

Elgaaly, M., Seshadri, A. and Hamilton, R.W. (1997), "Bending strength of steel beams with corrugated webs", *ASCE J. Struct. Eng.*, **123**(6), 772-782.

Hamilton, R.W. (1993), "Behavior of welled girder with corrugated webs", Ph.D. Dissertation, University of Maine, Maine, Canada

Hsu, T.T.C. (1984), *Torsion of Reinforced Concrete*, Van Nostrand Reinhold Company, New York, NY.

Hsu, T.T.C. (1988), "Softened truss model theory for shear and torsion", *ACI Struct. J.*, **85**(6), 624-635.

Karayannis, C.G. (2000), "Smeared crack analysis for plain concrete in torsion", *ASCE J. Struct. Eng.*, **126**(6), 638-645.

Karayannis, C.G. and Chalioris, C.E. (2000a). "Experimental validation of smeared analysis for plain concrete in torsion", *ASCE J. Struct. Eng.*, **126**(6), 646-653.

Karayannis, C.G. and Chalioris, C.E. (2000b). "Strength of prestressed concrete beams in torsion", *Struct. Eng. & Mech.*, **10**(2), 165-180.

Machimdamrong, C., Watanabe, E. and Utsunomiya, T. (2004), "Analysis of corrugated steel web girders by an efficient beam bending theory", *JSCE Struct. Eng. Earthq. Eng.*, **21**(2), 131-142.

Mo, Y.L., Jeng, C.H. and Chang, Y.S. (2000), "Torsional behavior of prestressed concrete box-girder bridges with corrugated steel webs", *ACI Struct. J.*, **97**(6), 849-859.

Mo, Y.L. and Fan, Y.L. (2006), "Torsional design of hybrid concrete box girders", *ASCE J. Bridge Eng.*, **11**(3), 329-339.

Moon, J., Yi, J., Choi, B.H. and Lee, H.E. (2009), "Lateral-torsional buckling of I-girder with corrugated webs under uniform bending", *Thin-Walled Struct.*, **47**, 21-30.

Moon, J., Yi, J., Choi, B.H. and Lee, H.E. (2009), "Shear strength and design of trapezoidally corrugated steel webs", *J. Constr. Steel Res.*, **65**, 1198-1205.

Samanta, A. and Mukhopadhyay, M. (1999), "Finite element static and dynamic analyses of folded plates", *Eng. Struct.*, **21**(3), 227-287.

Shima, H. and Watanabe, S. (2009), "Formulation for load-slip relationships of headed stud connector", *Proceedings of '2009 fib Symposium*, London, June.

Yi, J., Gil, H., Youm, K. and Lee, H.E. (2008), "Interactive shear buckling of trapezoidally corrugated webs", *Eng. Struct.*, **30**, 1659-1666.

CC